

Position Aided Beam Alignment for Millimeter Wave Backhaul Systems with Large Phased Arrays

George C. Alexandropoulos

Mathematical and Algorithmic Sciences Lab, France Research Center, Huawei Technologies France,
20 Quai du Point du Jour, 92100 Boulogne-Billancourt, France
email: george.alexandropoulos@huawei.com

Abstract—Consensus has been reached between wireless industry bodies and academia on the indispensability of network densification in meeting the throughput and coverage demands for fifth generation (5G) wireless networks. One of the major challenges with the current trend of dense multi-tier network deployments is the wireless backhauling of the various small cells. Recently, wireless backhaul communication has been largely realized with large antennas operating in the millimeter wave (mmWave) frequency band and implementing highly directional beamforming. In this paper, we focus on the alignment problem of narrow beams between fixed position network nodes in mmWave backhaul systems that are subject to small displacements due to wind flow or ground vibration. We consider nodes equipped with antenna arrays that are capable of performing only analog beamforming and communicate through wireless channels including a line-of-sight component. Aiming at minimizing the time needed to achieve beam alignment, we present an efficient method that capitalizes on the exchange of position information between the nodes to design their beamforming and combining vectors. Our representative numerical results on the outage probability with the proposed beam alignment method offer useful preliminary insights on the impact of some system and operation parameters.

Index Terms—Analog beamforming, antenna arrays, backhaul systems, beam alignment, combining, tracking, millimeter wave.

I. INTRODUCTION

Mobile communication in the millimeter wave (mmWave) frequency band [1] is a promising technology for addressing the high throughput requirement (at least 1 Gbps outdoors) for the fifth generation (5G) mobile communication networks [2], [3]. Short-range mmWave communication at the unlicensed band of 60 GHz is already standardized in IEEE 802.11ad [4] and initial theoretical investigations on mmWave cellular systems [1], [5] have identified their potentials together with their key challenges. The mmWave frequencies have been also recently considered as a possible solution for the wireless backhaul communication of small cells [6], [7], which are expected to be densely deployed as an efficient means for increasing the geographic spectrum reusability [8].

Reliable mmWave backhauling depends on very directional transmissions and receptions, which are implemented in practice either with antennas having large apertures or with large phased antenna arrays [6]. By exploiting the fact that the wavelength at very high frequencies is very small, large phased antennas can be cheaply packed into small form factors and, thus, have been effectively used in realizing highly directional

beamforming (BF) supporting long outdoor links. To achieve the full benefit from BF in a communication link between multi-antenna nodes, the entire channel state information needs to be available at both communication ends. However, this information is hard to acquire in mmWave systems due to the low coherence time, the radio frequency (RF) hardware limitations (a phased antenna array has a large number of antenna elements attached to one RF chain), and the small signal-to-noise ratio (SNR) before BF. Although very recent theoretical works [5], [9]–[11] capitalized on the spatial sparsity of mmWave channels [12] to estimate portions of the channel gain matrix, the presented approaches required lengthy training phases to estimate the channel in multiple directions using complex compressed sensing algorithms. Another family of approaches (e.g., [13]–[18]) for efficient BF is based on beam switching between the communicating nodes in order to find a pair of beams from their available codebooks meeting a predefined performance threshold. When such a beam pair is found, beam alignment is considered to be achieved and no further beam searching is needed. The two-stage exhaustive search BF protocol for medium access control adopted in the IEEE 802.11ad standard [4] is mainly based on the multi-sector BF technique of [13]. In [14], a two-sided beam alignment method that is based on multi-round exchanges of control information between the communicating nodes was presented. Multi-round beam searching techniques for initial channel access in mmWave systems have been also presented in [15]–[17] primarily intending at alleviating the exhaustive beam search delay issue. In [18], a beam searching method for mmWave backhaul systems with phased antenna arrays that is robust to random movements of the arrays was presented. Although the method avoids the costly exhaustive sampling of all pairs of transmit and receive beams using the hierarchical codebooks proposed therein, multi-round control information exchange for beam alignment is still needed.

In this paper, we focus on the mmWave backhaul system of [18] and present a robust beam alignment method for wireless channels including a line-of-sight (LOS) component. Since reducing the time needed to find an acceptable pair of beams frees up time for data transmission and reduces the probability of interfering to adjacent links, the proposed method intends at achieving beam alignment in at most two rounds of control information exchange. The core idea of the method lies on the control information, which is considered

to be the new position of the nodes after each declared beam misalignment event, on its exchange, and on its utilization in designing the BF and combining technique. By assuming that each node is equipped with a position sensor (various high sensitivity displacement sensors are available in civil engineering), a set of actions are first performed by one of the nodes serving as the master node. If needed, a set of actions follows by the other node that plays the role of the slave node, and finally, a second set of actions by the master node might be used. It is noted that positioning sensors have been also considered in [19], [20], however, they were adopted for identifying and circumventing beam misalignment only at the transmit node. By introducing a simple model that captures the small displacements of the antenna arrays of the nodes due to wind flow or ground vibration, we present representative performance evaluation results for the outage probability (OP) with the proposed beam alignment method for various system and operation parameters.

Notation: Vectors and matrices are denoted by boldface lowercase letters and boldface capital letters, respectively. The transpose and Hermitian transpose of a matrix \mathbf{A} are denoted by \mathbf{A}^T and \mathbf{A}^H , respectively, $\text{diag}\{\mathbf{a}\}$ denotes a square diagonal matrix with \mathbf{a} 's elements in its main diagonal, whereas \mathbf{I}_n ($n \geq 2$) is the $n \times n$ identity matrix. The i th element of \mathbf{a} and the (i, j) th element of \mathbf{A} are denoted by $[\mathbf{a}]_i$ and $[\mathbf{A}]_{i,j}$, respectively, and $\|\mathbf{A}\|_F$ gives the Frobenius norm of \mathbf{A} . \mathcal{C} represents the complex number set, $\text{card}(\mathcal{F})$ is the cardinality of set \mathcal{F} , $|\cdot|$ denotes the amplitude of a complex number, and $\mathbb{E}\{\cdot\}$ is the expectation operator. $d(M, N)$ denotes the length of the line segment connecting the points M and N . Notation $x \sim \mathcal{CN}(0, \sigma^2)$ indicates that x is a circularly-symmetric complex Gaussian random variable with zero mean and variance σ^2 , while $x \sim \mathcal{U}(\alpha, \beta)$ represents a uniformly distributed random variable in $[\alpha, \beta]$.

II. SYSTEM AND CHANNEL MODELS

The system model under investigation and the considered mmWave channel model are presented in the following. In this work, we assume that the system nodes are deployed in the plane, and we leave the extension for the three dimensions for the extended version of this paper.

A. System Model

Suppose the wireless backhaul communication system of Fig. 1 operating in the mmWave frequency band and consisting of two half duplex multi-antenna transceiver nodes A and B . As shown in the figure, the fixed positions of the nodes defines a Cartesian coordinate system, according to which the positions of nodes A and B at the time instant t are represented by the points $M_t^{(A)}$ and $M_t^{(B)}$, respectively. Their respective coordinates are $(0, 0)$ and $(0, d_t)$, where d_t denotes the physical distance between the nodes at this time instant. Regarding the mmWave access, each node is assumed to be equipped with one RF chain and is capable of realizing only analog transmit BF when being in transmit mode, and only analog receive combining when being in receive mode. Node

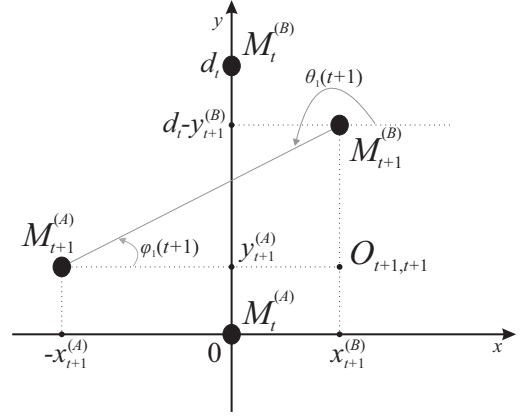


Fig. 1. The considered point-to-point wireless backhaul communication system. The positions of the nodes A and B at the time instant t are denoted by the points $M_t^{(A)}$ and $M_t^{(B)}$, respectively, and define a Cartesian coordinate system. At the time instant $t+1$ both nodes A and B move to new positions represented by the points $M_{t+1}^{(A)}$ and $M_{t+1}^{(B)}$, respectively. These new positions determine the coordinates of the point $O_{t+1,t+1}$; its first subscript refers to $M_{t+1}^{(A)}$ and the second to $M_{t+1}^{(B)}$.

A is assumed to have a large uniform linear antenna array (ULA) with N_A elements, whereas node B is equipped with a large N_B -element ULA. We hereinafter assume for simplicity that the positions of the nodes coincide with the positions of the centers of their antenna arrays.

To establish wireless communication between nodes A and B , i.e., meeting a minimum required performance threshold for reliable information exchange, a control phase for channel access is adopted. In particular, we assume that communication is realized in discrete time instants each including a control and a data phase. The control phase constitutes of several time slots during which data communication is being set up. We assume that during each discrete time instant the channel remains constant, but it may change between different instances. During the control phase for channel access, relevant information needs to be exchanged between nodes A and B . This control information exchange requires in general a much less stringent performance threshold than data exchange, and can be in principle handled by the considered communication systems. Another option would be to equip both nodes with a dedicated robust low frequency communication system intended exclusively for reliable control information exchange. It is adequate for this system to operate at very low data rate, and hence, it can be narrowband and realized with a single antenna at each node. Very recently, a method for mmWave beam alignment assisted by a radar system was presented in [21] for vehicular-to-infrastructure communication.

Before signal transmission from node A , the unit power data stream $s \in \mathcal{C}$ (chosen from a discrete modulation set) is processed by a BF vector $\mathbf{v}_A \in \mathcal{C}^{N_A \times 1}$, and upon signal reception at node B , the combining vector $\mathbf{u}_B \in \mathcal{C}^{N_B \times 1}$ is used for processing the received signal. Similarly, node B makes use of the BF vector $\mathbf{v}_B \in \mathcal{C}^{N_B \times 1}$ when transmitting, and node A utilizes the combining vector $\mathbf{u}_A \in \mathcal{C}^{N_A \times 1}$.

when being in receive mode. Due to practical limitations with the considered analog antenna arrays [5], [18], the analog antenna weights at both nodes are supposed to take values from discrete sets. In particular, we assume that \mathbf{v}_A and \mathbf{u}_A at node A are chosen from the finite set \mathcal{F}_A of predefined N_A -element vectors. The same holds for node B ; \mathbf{v}_B and \mathbf{u}_B belong to the finite set \mathcal{F}_B of predefined N_B -element vectors. Without loss of generality, it is assumed that for any $\mathbf{f} \in \mathcal{F}_A$ with $\mathbf{f} \in \mathcal{C}^{N_A \times 1}$ and any $\mathbf{z} \in \mathcal{F}_B$ with $\mathbf{z} \in \mathcal{C}^{N_B \times 1}$ holds $|\mathbf{f}|_i|^2 \triangleq N_A^{-1}$ with $i = 1, 2, \dots, N_A$ and $|\mathbf{z}|_j|^2 \triangleq N_B^{-1}$ with $j = 1, 2, \dots, N_B$. When node A transmits information to node B , the output signal of the combiner at node B can be mathematically expressed as

$$y_B = \sqrt{p} \mathbf{u}_B^H \mathbf{H}_{BA} \mathbf{v}_A s + \mathbf{u}_B^H \mathbf{n}_B, \quad (1)$$

where p is the transmit power, $\mathbf{H}_{BA} \in \mathcal{C}^{N_B \times N_A}$ denotes the channel gain matrix between nodes B and A , and $\mathbf{n}_B \in \mathcal{C}^{N_B \times 1}$ represents the zero-mean additive white Gaussian noise (AWGN) vector with covariance matrix $\sigma_B^2 \mathbf{I}_{N_B}$. The reverse link with node B transmitting and node A receiving can be similarly defined, and we assume that the forward channel \mathbf{H}_{BA} and the reverse channel are reciprocal, i.e., $\mathbf{H}_{AB} = \mathbf{H}_{BA}^H$.

B. Channel Model

A geometric channel model with L scatterers is adopted similar to [5], [12], where each scatterer contributes a single propagation path in the communication link between nodes B and A . We assume that during each discrete time instant the wireless channel remains constant, but it may change between different instances. According to this channel model, \mathbf{H}_{BA} included in (1) is expressed as

$$\mathbf{H}_{BA} = \mathbf{A}_B(\boldsymbol{\theta}) \text{diag}\{\mathbf{a}\} \mathbf{A}_A^H(\boldsymbol{\phi}), \quad (2)$$

where matrices $\mathbf{A}_A(\boldsymbol{\phi}) \in \mathcal{C}^{N_A \times L}$, with $\boldsymbol{\phi} \triangleq [\phi_1 \phi_2 \dots \phi_L]$, and $\mathbf{A}_B(\boldsymbol{\theta}) \in \mathcal{C}^{N_B \times L}$, with $\boldsymbol{\theta} \triangleq [\theta_1 \theta_2 \dots \theta_L]$, are defined as follows

$$\mathbf{A}_A(\boldsymbol{\phi}) \triangleq [\mathbf{a}_A(\phi_1) \mathbf{a}_A(\phi_2) \dots \mathbf{a}_A(\phi_L)], \quad (3a)$$

$$\mathbf{A}_B(\boldsymbol{\theta}) \triangleq [\mathbf{a}_B(\theta_1) \mathbf{a}_B(\theta_2) \dots \mathbf{a}_B(\theta_L)]. \quad (3b)$$

In (3), variable $\phi_\ell \in [0, 2\pi]$ with $\ell = 1, 2, \dots, L$ denotes the ℓ th path's angle of departure (AoD) from node A and variable $\theta_\ell \in [0, 2\pi]$ represents the ℓ th path's angle of arrival (AoA) at node B . Following the investigations in [22], we assume that the 1st channel path is a LOS one with energy much larger than each of the rest $L-1$ paths. In addition, $\mathbf{a}_A(\phi_\ell) \in \mathcal{C}^{N_A \times 1}$ and $\mathbf{a}_B(\theta_\ell) \in \mathcal{C}^{N_B \times 1}$ are the array response vectors at nodes A and B , respectively (for ULAs, these vectors are given by [5, eq. (5)]). In (2), $\mathbf{a} \in \mathcal{C}^{L \times 1}$ includes the path channel gains $\alpha_\ell \forall \ell = 1, 2, \dots, L$. We further assume that each path's amplitude is Rayleigh distributed and, in particular, that each $\alpha_\ell \sim \mathcal{CN}(0, N_A N_B P_L)$, where P_L denotes the average pathloss between nodes B and A .

In practical deployments of wireless backhaul systems, the antenna arrays of the communicating nodes are usually

mounted on outdoor structures that are exposed to wind flow and gusts. For example, picocell units are expected to be mounted on road signs and lampposts. These structures are susceptible to movement (or sway) due to wind or ground vibration, which might cause unacceptable OP if beam alignment is not frequently performed [18]. To capture the random movements of the antenna arrays at both nodes A and B in Fig. 1, we model the displacements at the x -axis and y -axis for both nodes A and B as

$$x^{(A)} \sim \mathcal{U}(-x_w^{(A)}, x_e^{(A)}), y^{(A)} \sim \mathcal{U}(-y_s^{(A)}, y_n^{(A)}), \quad (4a)$$

$$x^{(B)} \sim \mathcal{U}(-x_w^{(B)}, x_e^{(B)}), y^{(B)} \sim \mathcal{U}(y_s^{(B)}, y_n^{(B)}). \quad (4b)$$

In the latter expressions, $x_w^{(A)}$, $x_e^{(A)}$, $x_w^{(B)}$, and $x_e^{(B)}$ reveal the position limits in the x -axis for both nodes, while $y_s^{(A)}$, $y_n^{(A)}$, $y_s^{(B)}$, and $y_n^{(B)}$ represent their position limits in the y -axis. These limits disclose the tolerances of the structures hosting the antenna arrays and it is assumed that their values are much smaller than the physical distance of the nodes. Note that, in practice, the distribution of a node's position in certain time periods depends on the characteristics of the underlying phenomenon that caused the node's displacements within this period. Although the model in (4) is quite general, describing the worst case scenario of independent displacements at consecutive time instants, more sophisticated modeling of wind induced displacement (e.g., as in [18, Sec. III-B]) is left for future work.

III. POSITION AIDED BEAM ALIGNMENT

In this section, we first summarize the considered beam alignment design objective and then present a robust method suitable for mmWave backhaul communication systems operating over fading channels including a LOS component.

A. Design Objective

Suppose that at the time instant $t+1$ both nodes A and B move to new positions represented by the points $M_{t+1}^{(A)}$ and $M_{t+1}^{(B)}$, respectively, with respective coordinates $(x_{t+1}^{(A)}, y_{t+1}^{(A)})$ and $(x_{t+1}^{(B)}, y_{t+1}^{(B)})$, as shown in Fig. 1. According to the presented channel model in Sec. II-B, the channel between the receive node B and the transmit node A at the discrete time instant $t+1$ can be expressed as $\mathbf{H}_{BA}(t+1) = \mathbf{A}_B(\boldsymbol{\theta}(t+1)) \text{diag}\{\mathbf{a}(t+1)\} \mathbf{A}_A^H(\boldsymbol{\phi}(t+1))$, with $\boldsymbol{\phi}(t+1) \triangleq [\phi_1(t+1) \phi_2(t+1) \dots \phi_L(t+1)]$ and $\boldsymbol{\theta}(t+1) \triangleq [\theta_1(t+1) \theta_2(t+1) \dots \theta_L(t+1)]$ denoting the AoDs and AoAs, respectively, resulting from the new node positions, while $\mathbf{a}(t+1)$ includes their channel gains. The objective for beam alignment in this time instant is to design the BF vector at node A and the combining vector at node B as follows

$$\{\mathbf{v}_A(t+1), \mathbf{u}_B(t+1)\} = \max_{\mathbf{f} \in \mathcal{F}_A, \mathbf{z} \in \mathcal{F}_B} |\mathbf{z}^H \mathbf{H}_{BA}(t+1) \mathbf{f}|^2. \quad (5)$$

If perfect knowledge of $\mathbf{H}_{BA}(t+1)$ was available at both nodes, it is well known [23] that nodes A and B should use the principal left and right singular vectors of $\mathbf{H}_{BA}(t+1)$ as the

BF and combining vectors, respectively, to maximize the BF gain. However, neither $\mathbf{H}_{BA}(t+1)$ for any t can be estimated at any of the nodes due to the assumed hardware limitations nor the nodes are capable of realizing any arbitrary vector. Therefore, latest approaches [13]–[18] rely on beam searching within the available sets \mathcal{F}_A and \mathcal{F}_B , aiming at achieving beam alignment with as much as possible reduced control signaling overhead.

B. Proposed Method

Let us consider that, upon installation of the mmWave backhaul system of Fig. 1 at the initial discrete time instant t , both nodes A and B are aware of the coordinate system defined by the coordinates of the points $M_t^{(A)}$ and $M_t^{(B)}$. In the next discrete time instant $t+1$, suppose that both nodes move to the new position points $M_{t+1}^{(A)}$ and $M_{t+1}^{(B)}$, as shown in the same figure. Each node's displacement in the x and y axes is assumed to be available to the node (through, for example, dedicated high sensitivity displacement sensors). The latter indicates that each node is aware of the coordinates of its new position, i.e., node A learns the coordinates $(x_{t+1}^{(A)}, y_{t+1}^{(A)})$ and B obtains $(x_{t+1}^{(B)}, d_t - y_{t+1}^{(B)})$. If also the coordinates of the position of node B become available to A (through, for example, a dedicated control channel), then the latter node may estimate the AoD of the LOS channel path for its transmission at this time instant as

$$\hat{\phi}_1(t+1) = \begin{cases} \arcsin(g_{t+1}), & x_{t+1}^{(B)} \geq x_{t+1}^{(A)} \\ \pi - \arcsin(g_{t+1}), & x_{t+1}^{(B)} < x_{t+1}^{(A)} \end{cases}, \quad (6)$$

where the positive real g_{t+1} is given by

$$g_{t+1} = \frac{d(O_{t+1,t+1}, M_{t+1}^{(B)})}{d(M_{t+1}^{(A)}, M_{t+1}^{(B)})}. \quad (7)$$

From the specific nodes' positions in Fig. 1 at time $t+1$ yields

$$g_{t+1} = \frac{d_t - y_{t+1}^{(A)} - y_{t+1}^{(B)}}{\sqrt{(x_{t+1}^{(A)} + x_{t+1}^{(B)})^2 + (d_t - y_{t+1}^{(A)} - y_{t+1}^{(B)})^2}}. \quad (8)$$

In a similar way, if node A shares its coordinates at the same time instant with B , then node B can estimate the AoA of the LOS path for A 's transmission as

$$\hat{\theta}_1(t+1) = \begin{cases} \pi + \phi_1(t+1), & x_{t+1}^{(B)} \geq x_{t+1}^{(A)} \\ 2\pi - \phi_1(t+1), & x_{t+1}^{(B)} < x_{t+1}^{(A)} \end{cases}. \quad (9)$$

The AoD and AoA of the LOS path can be obtained similarly if node B transmits and node A operates in receive mode.

Capitalizing on (6) and on the considered channel model for each time instant $t+1$, we propose that the transmit node A utilizes its available estimate $\hat{\phi}_1(t+1)$ to realize a beam that steers towards the direction of the receive node B . To accomplish this, it searches inside its available beam codebook \mathcal{F}_A for the vector that is closest to $\mathbf{a}_A(\hat{\phi}_1(t+1))$.

In mathematical terms, node A designs its BF vector at each time instant $t+1$ as

$$\mathbf{v}_A(t+1) = \min_{\mathbf{f} \in \mathcal{F}_A} \left\| \mathbf{f} - \mathbf{a}_A(\hat{\phi}_1(t+1)) \right\|_{\text{F}}^2. \quad (10)$$

Similarly, receive node B uses its available estimate $\hat{\theta}_1(t+1)$ at each time instant $t+1$ to realize a beam as close as possible to the direction of the node A . Therefore, this node constructs its combining vector as

$$\mathbf{u}_B(t+1) = \min_{\mathbf{z} \in \mathcal{F}_B} \left\| \mathbf{z} - \mathbf{a}_B(\hat{\theta}_1(t+1)) \right\|_{\text{F}}^2. \quad (11)$$

By using the vectors given by (10) and (11) at nodes A and B , respectively, the instantaneous received SNR at node B is calculated as

$$\gamma_{t+1} = \frac{p}{\sigma_B^2} |\mu_{t+1}|^2, \quad (12)$$

where $\mu_{t+1} \in \mathcal{C}$ is defined as

$$\mu_{t+1} = \sum_{\ell=1}^L \alpha_{\ell}(t+1) \mathbf{u}_B^{\text{H}}(t+1) \mathbf{a}_B(\hat{\theta}_{\ell}(t+1)) \times \mathbf{a}_A^{\text{H}}(\hat{\phi}_{\ell}(t+1)) \mathbf{v}_A(t+1). \quad (13)$$

Note that for the special case of $L = 1$, perfectly estimated AoD and AoA for the LOS path, and infinite resolution beam codebooks at both nodes yields $\mu_{t+1} = \alpha_1(t+1)$. This indicates that for this ideal case the vectors given by (10) and (11) maximize the BF gain described in (5), and equivalently the SNR given by (12).

The proposed beam alignment method is summarized in Algorithm 1. Although the method is presented with node A being the transmitter and node B the receiver, it can be evenly used for the case where nodes exchange roles. According to Algorithm 1, beam alignment is considered to be achieved when the instantaneous SNR of the communication link, measured either by node A during its set of actions or during the actions of node B , is greater or equal to a minimum required SNR γ_o for data communication. Note also that the method includes three separate phases: i) the *Node A Recovery Phase 1*; ii) the *Node B Recovery Phase*; and iii) the *Node A Recovery Phase 2*. When beam alignment is achieved with only the *Node A Recovery Phase 1*, no control signaling is needed to be exchanged between the nodes. One control signal is needed to be sent from node A to B when beam alignment is accomplished within the actions inside the *Node A Recovery Phase 1* and *Node B Recovery Phase*. Finally, when all phases are utilized, two control signals are required; the previously described and the one from node B to A .

IV. NUMERICAL RESULTS AND DISCUSSION

In this section we evaluate the performance of the proposed beam alignment method presented in Sec.III-B over the presented mmWave channel model in Sec.II-B. In particular, we evaluate the OP performance defined as the probability that the instantaneous SNR falls below a minimum SNR threshold γ_o . To carry out this evaluation, we have simulated

Algorithm 1 Position Aided Beam Alignment

Initialization: Construct the coordinate system of Fig. 1 upon the installation of nodes A and B at the initial time instant t . Determine the minimum required SNR γ_o for data communication.

1: **for** $n = t + 1, t + 2, \dots$ **do**

Node A Recovery Phase 1:

2: **if** $\gamma_n \geq \gamma_o$, **then**

3: Set $\mathbf{v}_A(n) = \mathbf{v}_A(n-1)$, $\mathbf{u}_B(n) = \mathbf{u}_B(n-1)$, and transmit data.

4: **else**

5: Obtain the coordinates of the new position $M_n^{(A)}$.
 6: Compute the AOD $\hat{\phi}_1(n)$ using (6) and the coordinates of the positions $M_n^{(A)}$ and $M_{n-1}^{(B)}$, and the point $O_{n,n-1}$.

7: Compute $\mathbf{a}_A(\hat{\phi}_1(n))$ and design $\mathbf{v}_A(n)$ using (10).

8: **end if**

9: **if** $\gamma_n \geq \gamma_o$ **then**

10: Set $\mathbf{v}_A(n)$ as in step 7, $\mathbf{u}_B(n) = \mathbf{u}_B(n-1)$, and transmit data.

11: **else**

12: Send the coordinates of $M_n^{(A)}$ to Node B .

13: **end if**

Node B Recovery Phase:

14: Upon reception of a control signal with the coordinates of $M_n^{(A)}$, obtain the coordinates of $M_n^{(B)}$.

15: Compute the AOA $\hat{\theta}_1(n)$ using (9) and the coordinates of the positions $M_n^{(A)}$ and $M_n^{(B)}$, and $O_{n,n}$.

16: Compute $\mathbf{a}_B(\hat{\theta}_1(n))$ and design $\mathbf{u}_B(n)$ using (11).

17: **if** $\gamma_n \geq \gamma_o$, **then**

18: Trigger node A to transmit data.

19: Set $\mathbf{v}_A(n)$ as in step 7, $\mathbf{u}_B(n)$ as in step 16, and transmit data.

20: **else**

21: Send the coordinates of $M_n^{(B)}$ to Node A and use $\mathbf{u}_B(n)$ designed in step 16.

22: **end if**

Node A Recovery Phase 2:

23: Upon reception of a control signal with the coordinates of $M_n^{(B)}$, compute the AOD $\hat{\phi}_1(n)$ using (6) and the coordinates of $M_n^{(A)}$ and $M_n^{(B)}$, and $O_{n,n}$.

24: Compute $\mathbf{a}_A(\hat{\phi}_1(n))$ and design $\mathbf{v}_A(n)$ using (10).

25: Set $\mathbf{v}_A(n)$ as in step 23, $\mathbf{u}_B(n)$ as in step 16, and transmit data.

26: **end for**

10^4 channel samples according to (2) with normalized σ_B^2 and $P_L = d_1^{-3.75}$, where each channel sample appears at one discrete time instant. We have considered Ricean fading channels with the κ -factor denoting the ratio of the energy in the LOS channel path to the sum of the energies in the other non LOS paths [22]. The distance of the nodes A and B at the initial time instant $t = 1$ is assumed to be $d_1 = 10\text{m}$ and the random displacements of the nodes

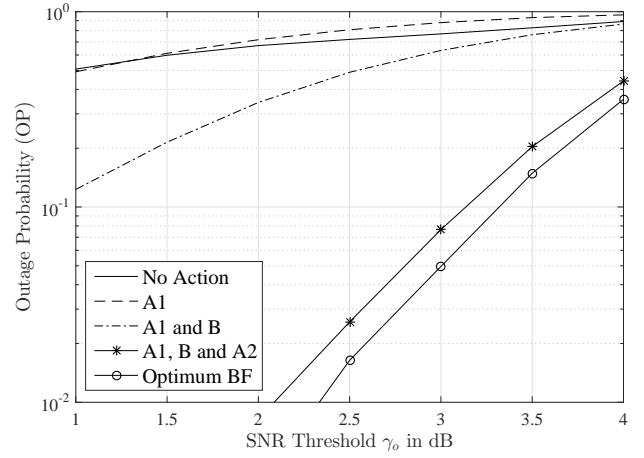


Fig. 2. OP versus the SNR threshold γ_o in dB for $N_A = N_B = 32$, $p = 5\text{dB}$, $\text{card}(\mathcal{F}_A) = \text{card}(\mathcal{F}_B) = 33$, $\kappa = 20\text{dB}$, and different phases of the proposed method. Curves for the unfeasible optimum BF case and the case of no action for beam alignment are included.

in the x -axis and y -axis due to wind gusts are obtained from (4) with $x_w^{(A)} = x_e^{(A)} = x_w^{(B)} = x_e^{(B)} = 1.5\text{m}$ and $y_w^{(A)} = y_e^{(A)} = y_w^{(B)} = y_e^{(B)} = 1.5\text{m}$. The beam codebooks \mathcal{F}_A and \mathcal{F}_B are constructed by quantizing the feasible sets of departure and arrival angles, respectively. Specifically, each i th BF vector belonging in \mathcal{F}_A with $i \in \text{card}(\mathcal{F}_A)$ is given by

$$\mathbf{f}_i = \frac{1}{\sqrt{N_A}} [1 \ e^{-j2\pi d_\lambda \cos(\chi_i)} \ \dots \ e^{-j2\pi d_\lambda (N_A-1) \cos(\chi_i)}]^T,$$

where d_λ denotes the spacing between adjacent antenna elements in wavelengths and the departure angle χ_i takes discrete values with step size $2^{1-q}(\chi_{\max} - \chi_{\min})$ within $[\chi_{\min}, \chi_{\max}]$, where q represents the number of angle quantization bits. Each j th combining vector inside \mathcal{F}_B with $j \in \text{card}(\mathcal{F}_B)$ is constructed in a similar way to \mathcal{F}_A with each arrival angle $\psi_j \in [\psi_{\min}, \psi_{\max}]$ being quantized with q bits. In the following plots, we have set $\chi_{\min} = 60^\circ$, $\chi_{\max} = 120^\circ$, $\psi_{\min} = 240^\circ$, and $\psi_{\max} = 300^\circ$ with respect to the nodes' orientation in Fig. 1.

In Figs. 2 and 3 the OP with the proposed beam alignment method is depicted as a function of the SNR threshold γ_o in dB for the transmit power $p = 5\text{dB}$ and two different scenarios. In the scenario for Fig. 2, it is considered that $N_A = N_B = 32$, $\text{card}(\mathcal{F}_A) = \text{card}(\mathcal{F}_B) = 33$ resulting from $q = 6$, and the Ricean factor $\kappa = 20\text{dB}$. In Fig. 3, we considered a scenario where $N_A = N_B = 16$, $\text{card}(\mathcal{F}_A) = \text{card}(\mathcal{F}_B) = 17$ resulting from $q = 5$, and the Ricean factor $\kappa = 13.2\text{dB}$. In both figures, the OP curves for the case of no action for beam alignment and the case of optimum BF [23] when perfect channel knowledge is available were sketched. As for the proposed method, the performance for different sequences of phases is also demonstrated. In particular, we provide the performance for the case where only *Node A Recovery Phase 1* is used, denoted by A1; the case where *Node A Recovery Phase 1* followed by *Node B Recovery Phase* are used, denoted by A1 and B; and the case where all phases are utilized, denoted

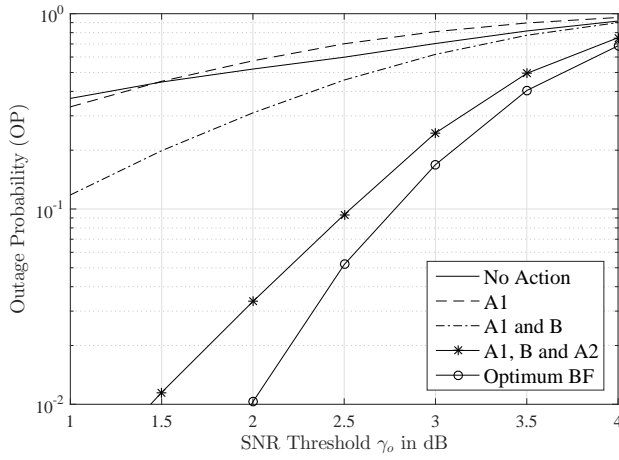


Fig. 3. OP versus the SNR threshold γ_o in dB for $N_A = N_B = 16$, $p = 5$ dB, $\text{card}(\mathcal{F}_A) = \text{card}(\mathcal{F}_B) = 17$, $\kappa = 10$ dB, and different phases of the proposed method. Curves for the unfeasible optimum BF case and the case of no action for beam alignment are included.

by A1, B and A2. As seen from both figures and as expected, OP degrades with increasing γ_o . It is also shown that the exchange of position information improves this probability for any γ_o value. In fact, the availability of nodes' position at both nodes, with only 2 control signals according to the proposed method, results in the best performance. Evidently, actions from only the transmitter or exchange of only the latter's position information result in poor OP. Combining Figs. 2 and 3, it can be concluded that the OP performance after 2 control signals approaches that of the optimum BF as the resolution of the available codebooks increases and the LOS component of the wireless channel becomes more dominant.

We have also compared the proposed beam alignment method with an exhaustive beam search similar to [15] that seeks to find the first beam pair meeting γ_o whenever beam misalignment occurs. For the parameter settings of Fig. 3 we quote the following representative results: *i*) the proposed method achieves 98% of the average received SNR of optimum BF irrespective of γ_o , while the exhaustive search only the 28% for $\gamma_o = 1$ dB after 30 control signals on average; and *ii*) for $\gamma_o = 3$ dB the exhaustive search reaches the 72% of the optimum BF SNR requiring on average 153 control signals.

V. CONCLUSION

In this paper, we investigated the problem of beam alignment between network nodes in wireless backhaul communication systems operating in the mmWave frequency band. We considered the practical case of random movement of the large phased arrays of the nodes due to wind flow or ground vibration, and presented a simple model that captures their small displacements. A robust beam alignment method for environments including a LOS component was presented that capitalizes on the exchange of position information between the nodes to design their BF and combining vectors. Through representative OP performance evaluation results the impact of some key parameters on the performance of the

proposed method was highlighted. Future directions include the performance analysis of the method under realistic antenna patterns and codebooks as well as imperfections (e.g., sensor measurement inaccuracies). We also intend at incorporating direction finding techniques into the proposed method in order to tackle efficient beam alignment under non LOS conditions.

REFERENCES

- [1] T. S. Rappaport *et al.*, "Millimeter wave mobile communications for 5G cellular: It will work!" *IEEE Access*, vol. 1, pp. 335–349, May 2013.
- [2] F. Boccardi *et al.*, "Five disruptive technology directions for 5G," *IEEE Commun. Mag.*, vol. 52, no. 2, pp. 74–80, Feb. 2014.
- [3] J. G. Andrews *et al.*, "What will 5G be?" *IEEE J. Sel. Areas Commun.*, vol. 32, no. 6, pp. 1065–1082, Jun. 2014.
- [4] "IEEE wireless LAN MAC and PHY specifications— Amendment 3: Enhancements for very high throughput in the 60 GHz band," *IEEE Std. 802.11ad*, 2012.
- [5] A. Alkhateeb *et al.*, "Channel estimation and hybrid precoding for millimeter wave cellular systems," *IEEE J. Sel. Topics Signal Process.*, vol. 8, no. 5, pp. 831–846, Oct. 2014.
- [6] S. Chia *et al.*, "The next challenge for cellular networks: Backhaul," *IEEE Microwave Mag.*, vol. 10, no. 5, pp. 54–66, Aug. 2009.
- [7] X. Ge *et al.*, "5G wireless backhaul networks: Challenges and research advances," *IEEE Netw.*, vol. 28, no. 6, pp. 6–11, Dec. 2014.
- [8] N. Bhushan *et al.*, "Network densification: The dominant theme for wireless evolution into 5G," *IEEE Commun. Mag.*, vol. 52, no. 2, pp. 82–89, Feb. 2014.
- [9] Z. Marzi *et al.*, "Compressive channel estimation and tracking for large arrays in mm-wave picocells," *IEEE Trans. Signal Process.*, vol. 11, no. 3, pp. 514–527, Apr. 2016.
- [10] A. Bazzi *et al.*, "A comparative study of sparse recovery and compressed sensing algorithms with application to AoA estimation," in *Proc. IEEE SPAWC*, Edinburgh, UK, 3–6 Jul. 2016, pp. 1–5.
- [11] G. C. Alexandropoulos and S. Chouvardas, "Low complexity channel estimation for millimeter wave systems with hybrid A/D antenna processing," in *Proc. IEEE GLOBECOM*, Washington D.C., USA, 4–8 Dec. 2016, pp. 1–6.
- [12] H. Zhang *et al.*, "Channel modeling and MIMO capacity for outdoor millimeter wave links," in *Proc. IEEE WCNC*, Sydney, Australia, 18–21 Apr. 2010, pp. 1–6.
- [13] K. Hosoya *et al.*, "Multiple sector ID capture (MIDC): A novel beamforming technique for 60 GHz band multi-Gbps WLAN/PAN systems," *IEEE Trans. Antennas Propag.*, vol. 63, no. 1, pp. 81–96, Jan. 2015.
- [14] J. Wang *et al.*, "Beam codebook based beamforming protocol for multi-Gbps millimeter-wave WPAN systems," *IEEE J. Sel. Areas Commun.*, vol. 27, no. 8, pp. 1390–1399, Oct. 2009.
- [15] C. Jeong *et al.*, "Random access in millimeter-wave beamforming cellular networks: Issues and approaches," *IEEE Commun. Mag.*, vol. 53, no. 1, pp. 180–185, Jan. 2015.
- [16] C. Barati *et al.*, "Directional cell discovery in millimeter wave cellular networks," *IEEE Trans. Wireless Commun.*, vol. 14, no. 12, pp. 6664–6678, Dec. 2015.
- [17] V. Raghavan *et al.*, "Beamforming tradeoffs for initial UE discovery in millimeter-wave mimo systems," *IEEE J. Sel. Topics Signal Process.*, vol. 10, no. 3, pp. 543–559, Apr. 2016.
- [18] S. Hur *et al.*, "Millimeter wave beamforming for wireless backhaul and access in small cell networks," *IEEE Trans. Commun.*, vol. 61, no. 10, pp. 4391–4403, Oct. 2013.
- [19] R. Maiburger *et al.*, "Location based beamforming," in *Proc. IEEE IEEEI*, Eliat, Israel, 17–20 Nov. 2010, pp. 184–187.
- [20] A. W. Doff, K. Chandra, and R. V. Prasad, "Sensor assisted movement identification and prediction for beamformed 60 GHz links," *available on ArXiv.org*, 2015.
- [21] N. González-Prelcic *et al.*, "Radar aided mmwave beam alignment in V2I communications supporting antenna diversity," in *Proc. IEEE ITA*, San Diego, USA, 31 Jan.–2 Feb. 2016, pp. 1–7.
- [22] Z. Muhi-Eldeen *et al.*, "Modelling and measurements of millimetre wavelength propagation in urban environments," *IET Microwaves, Ant. Propag.*, vol. 4, no. 9, pp. 1300–1309, May 2010.
- [23] D. J. Love and R. W. Heath, Jr., "Equal gain transmission in multiple-input multiple-output wireless systems," *IEEE Trans. Commun.*, vol. 51, no. 7, pp. 1102–1110, Jul. 2003.